DNA Repair 12 (2013) 257–264

Contents lists available at SciVerse ScienceDirect

DNA Repair

journal homepage: www.elsevier.com/locate/dnarepair

Mismatch recognition function of *Arabidopsis thaliana* MutSγ

Rodrigo Gómez, Claudia P. Spampinato*

Centro de Estudios Fotosintéticos y Bioquímicos (CEFOBI), Facultad de Ciencias Bioquímicas y Farmacéuticas, Universidad Nacional de Rosario, Suipacha 531, 2000 Rosario, Argentina

ARTICLE INFO

Article history:
Received 6 December 2012
Received in revised form 9 January 2013
Accepted 10 January 2013
Available online 4 February 2013

Keywords:
Mismatch repair
Genome stability
Mutation rate
Arabidopsis thaliana
Saccharomyces cerevisiae

ABSTRACT

Genetic stability depends in part on an efficient DNA lesion recognition and correction by the DNA mismatch repair (MMR) system. In eukaryotes, MMR is initiated by the binding of heterodimeric MutS homologue (MSH) complexes, MSH2–MSH6 and MSH2–MSH3, which recognize and bind mismatches and unpaired nucleotides. Plants encode another mismatch recognition protein, named MSH7. MSH7 forms a heterodimer with MSH2 and the protein complex is designated MutSγ. We here report the effect the expression of Arabidopsis MSH2 and MSH7 alone or in combination exert on the genomic stability of *Saccharomyces cerevisiae*. AtMSH2 and AtMutSγ proteins failed to complement the hypermutator phenotype of an *msh2* deficient strain. However, overexpressing AtMutSγ in MMR proficient strains generated a 4-fold increase in *CAN1* forward mutation rate, when compared to wild-type strains. Can^r mutation spectrum analysis of AtMutSγ overproducing strains revealed a substantial increase in the frequency of base substitution mutations, including an increased accumulation of base pair changes from G:C to A:T and T:A to C:G, G:C or A:T. Taken together, these results suggest that AtMutSγ affects yeast genomic stability by recognizing specific mismatches and preventing correction by yeast MutSα and MutSβ, with subsequent inability to interact with yeast downstream proteins needed to complete MMR.

1. Introduction

DNA mismatch repair (MMR) system maintains genome stability by correcting single base–base mismatches and unpaired nucleotides in template or nascent DNA strands (deletion or insertion loops, respectively). Proteins involved in this pathway have been conserved from bacteria to plants [1] although both the nature and number of orthologues have become more complex throughout evolution. MutS and MutL proteins function as homodimers in *Escherichia coli* and as multiple heterodimers (mainly MutSα, MutSβ and MutLα) in yeast and humans. In addition, plants contain a unique MutS protein named MutSγ.

MutSα, MutSβ and MutSγ are heterodimers of MSH2 complexed with MSH6, MSH3 or MSH7, respectively [2–5]. MutSα is mainly required to correct single mispairs and short insertion/deletion loops (IDLs), whereas MutSβ is predominantly involved in the removal of large IDLs (2–12 nucleotides) [2,4,6,7]. Cristal structures of human MutSα in complex with a series of DNA substrates [8] confirmed the responsible motifs for mismatch recognition, previously observed in prokaryotic proteins [8–10]. A conserved FXE motif, only present in the MSH6 subunit, plays critical roles in mismatch interaction. MSH3 lacks these conserved phenylalanine and glutamate residues suggesting that protein binding to IDLs occurs through different contacts [11].

MutSγ is by far much less characterized than MutSα and MutSβ. So far, studies performed with AtMSH2 and AtMSH7 proteins, products of *in vitro* transcription and translation techniques, have suggested that MutSγ preferentially recognizes certain base–base mismatches [5,12]. In addition, MutSγ has a specific role in meiotic recombination [13,14]. In fact, MSH7, as well as MSH6 and prokaryotic MutS, contains the conserved FXE motif required for mismatch interaction [1]. To further characterize the *in vivo* role of MutSγ, we performed functional analyses in yeast. We used three chromosomal markers, in particular *his7-2*, *lys2::InsE-A$_{14}$* and *CAN1*. The *his7-2* allele, contains a T:A deletion in a stretch of 8 T:A in the *HIS7* gene [15]. Frameshift reversion, largely due to +1 bp insertions and −2 bp deletions, is evaluated by cell growth on medium lacking histidine. The second marker used, the allele *lys2*, contains a mononucleotide run of 14 As in the *LYS2* gene (*lys2::InsE-A$_{14}$*) [16]. Reversion by −1 bp deletions of the *lys2* allele enables the strain to grow on medium lacking lysine. Finally, the *CAN1* gene codes for arginine permease. This protein transports arginine and its toxic analog canavanine into the cell. When inactivating mutations, such as base substitutions, deletions, insertions, and large chromosomal rearrangements, occur in the *CAN1* gene, strains lose permease activity and become resistant to media containing canavanine [17].

Our data show that AtMSH2 is unable to complement the hypermutator phenotype of an *msh2* deficient strain. However, expression of AtMSH2–AtMSH7 protein complex in a MMR

* Corresponding author. Tel.: +54 341 4371955x113; fax: +54 341 54 341 4371955x103.
E-mail address: spampinato@cefobi-conicet.gov.ar (C.P. Spampinato).

1568-7864/$ – see front matter © 2013 Elsevier B.V. All rights reserved.
http://dx.doi.org/10.1016/j.dnarep.2013.01.002

Table 1
Primers used for vector constructions. Restriction sites and the ATG initiation codon are in italics and underlined, respectively.

Name	Sequence
y5pSac-MSH7	ATCT*GAGCTC*ACC<u>ATG</u>GTGCAGCGCCAGAGAT
y3pSph-MSH7	CGTG*GCATGC*TTATTTGGGAACACAGTAAGAGG
y5pKpn-MSH2	CG*CGGTACC*<u>ATG</u>GAGGGTAATTTCGAGGAA
y3pCsp-MSH2	CTACAT*CGGTCCG*TTATCACAGAAACTGCCT

proficient strain leads to a clear increase in *CAN1* mutator rate, indicating that the expression of the plant DNA repair protein affects yeast MMR mechanism. Analysis of Can^r mutation spectrum indicate a high frequency of G:C to A:T, T:A to G:C, T:A to C:G and T:A to A:T base substitutions. These studies suggest that MutSγ is important in ensuring genome stability by recognizing mismatches that arise by spontaneous deamination or environmental stresses, such as solar UV light and reactive oxygen species.

2. Materials and methods

2.1. Yeast strains and growth conditions

Saccharomyces cerevisiae haploid strains E134 (*MATα ade5 lys2::InsEA$_{14}$ trp1-289 his7-2 leu2-3, 112 ura3-52*) and DAG60 (*msh2*Δ derivative of E134) have been previously described [18]. Yeast were grown in YPDA [1% (w/v) yeast extract, 2% (w/v) peptone, 2% (w/v) glucose, 20 mg/l adenine] or SC [19] containing 2% (w/v) glucose without leucine (SCDL). When appropiate, 2% (w/v) galactose was included instead of glucose (SCGL) for inducing genes cloned downstream *GAL1-10* promoters. To measure forward mutation rates to canavanine resistance, SC medium without arginine containing 60 mg/l L-canavanine was used. Solid media were also supplemented with 1.5% (w/v) agar.

2.2. Vector constructions

Yeast expression plasmids were constructed in YEp181SPGAL [18] as follows. At*MSH7* was PCR amplified by the proofreading Vent DNA polymerase using the pGEM3Z-AtMSH7 plasmid [5] as template and the y5pSac-MSH7 and y3pSph-MSH7 oligonucleotides as primers (Table 1). PCR reactions were carried out as described by Gomez et al. [23] except elongation time was increased up to 3.5 min. The At*MSH7* gene was then inserted into the YEp181SPGAL vector after digestion with *Sac*I and *Sph*I. This construction places the At*MSH7* coding sequence downstream the *GAL1* promoter, generating the YEp-AtMSH7 plasmid (Fig. 1). Then, the At*MSH2* was inserted into this plasmid downstream the *GAL10* promoter as follows. The At*MSH2* sequence was amplified by PCR using the above conditions except for the template (pGEM3Z-AtMSH2, [20]) and primers used (y5pKpn-MSH2 and y3pCsp-MSH2, Table 1). The PCR fragment was digested with *Kpn*I and *Csp*I and ligated into the digested *Kpn*I/*Pst*I YEp-AtMSH7 plasmid. The resulting linear vector was then blunt-ended with Klenow DNA polymerase and afterwards ligated to generate YEp-AtMSH7/AtMSH2 plasmid (Fig. 1). Finally, the At*MSH7* gene was released from the YEp-AtMSH7/AtMSH2 plasmid by digestion with *BamH*I and *Sph*I followed by blunt-ended ligation. The resulting construction, named YEp-AtMSH2, contains the At*MSH2* cDNA downstream the *GAL10* promoter (Fig. 1). The absence of random mutations introduced by the DNA polymerase in all the PCR amplified fragments was determined by DNA sequencing (Macrogen, Korea).

2.3. Expression of MMR proteins

For MMR protein expression in yeast strains, electrocompetent cells were prepared and transformed as described previously [21] with some modifications. The electroporated cells were diluted in 1 ml YPDA and maintained 1 h at 30 °C without agitation. The cells were collected by centrifugation at 3000 × *g* for 3 min and the resulting pellet was resuspended in 50 μl of SCDL and spread on SCDL plates. Transformant colonies appeared within 3–4 days at 30 °C. Single colonies were grown in liquid SCDL media overnight at 30 °C. An aliquot of the culture was harvested and washed three times with distilled water to remove glucose medium. Cells were then inoculated into SCGL medium to give an initial $OD_{600\,nm} < 0.01$ and allowed to grow until an $OD_{600\,nm}$ of 0.2–0.3 was reached. Cells were harvested and immediately stored at −70 °C.

2.4. Yeast extract preparation

Cells ($2–3 \times 10^8$) were resuspended in 0.1 ml buffer containing 40 mM Tris–HCl, 1 mM EDTA, 1 mM PMSF, 0.1% (v/v) β-mercaptoethanol, pH 6.8. For denaturing extract preparation, buffer was also supplemented with 5% (w/v) SDS. Glass beads were added and 6 series of 1 min vortex-mixing alternating with 1 min incubation on ice were performed. After cell-lysis, samples were centrifuged in order to pellet glass beads and cell debris. The supernatants were stored at −70 °C.

2.5. Immunological analyses

Denaturing gels containing 50 μg of yeast extract were electrotransferred to nitrocellulose membranes (Bio-Rad) at 50 V for 1 h for immunoblotting [22]. Affinity purified anti-AtMSH2 polyclonal antibodies (6.5 μg/ml) were used for detection [23]. Bound primary antibodies were recognized by goat anti-rabbit IgG conjugated to alkaline phosphatase and subsequently developed with 5-bromo-4-chloro-3-indolyl phosphate and nitro blue tetrazolium [22].

2.6. Mutation rate measurement

Reversion rates of *lys2::InsEA$_{14}$* and *his7-2* and forward mutations to canavanine resistance were measured by fluctuation analysis as previously described [18,24]. Briefly, a single colony carrying a particular vector was grown to saturation in SCDL. Cultures were pelleted, washed twice in sterile distilled water to remove glucose, inoculated into the SCGL medium such that the initial inoculum size contained 1000 cells/ml, and dispensed (200 μl) into 96-well plates. Cultures were grown to saturation at 30 °C without shaking. Cells from 12 to 24 cultures were pooled and diluted to determine growth by measuring $OD_{600\,nm}$ and by plating into SCDL agar medium. Cells from 12 to 36 cultures were plated after appropriate dilutions onto selective medium lacking lysine or histidine to count for revertant mutants or lacking arginine but containing canavanine to count resistant mutants. Data were analyzed by the Lea-Coulson method of the median using the Fluctuation anALysis CalculatOR program [25]. The 95% confidence intervals were determined as previously described [26,27] while the significance of differences between mutation rates (*p*-value) was estimated using Kruskal–Wallis and Mann–Whitney tests, where appropriate.

2.7. DNA annealing and labeling

Oligodeoxyribonucleotides were purchased from Integrated DNA Technologies. A 61-bp G-T heteroduplex was prepared by mixing equal concentrations of top strand (5′-TCGCCAGAATCGCCGAATTGCTAGCAAGCTTTCGAGTCTAGAAATTCGGCGAATCCCGTCA-3′)

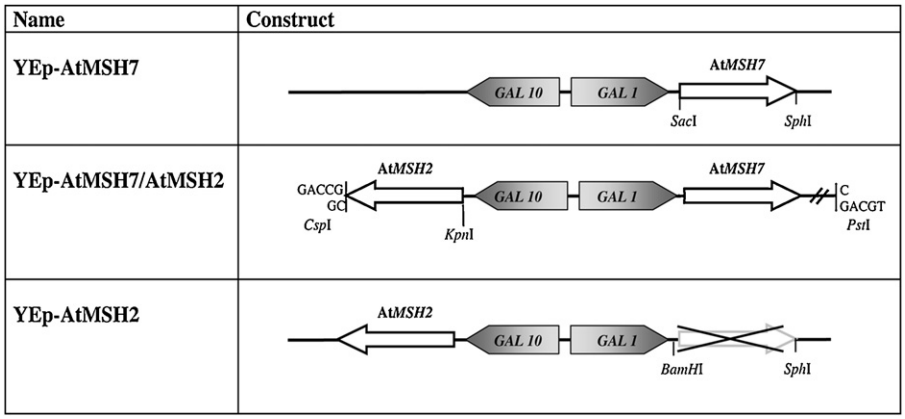

Fig. 1. Diagrams of reporter constructs. Both AtMSH2 and AtMSH7 coding sequences were cloned in YEp181SPGAL shuttle vectors. The cloning procedure is schematically represented and detailed under Section 2. The At*MSH2* and At*MSH7* genes and the *GAL1* and *GAL10* promoters are indicated and displayed as white or gray arrows, respectively. Key restriction enzyme sites and cloning strategy are also shown.

with bottom strand (5′-TGACGGGATTCGCCGAATTTCTAGACTCGA-GAGCTTGCTAGCAATTCGGCGATTCTGGCGA-3′). The reaction mix was heated in a Perkin-Elmer Gene Amp PCR System 2400 thermocycler at 94 °C for 2 min, 72 °C for 2 min, 55 °C for 2 min and 15 °C for 10 min. The heteroduplex (250 ng) was then end-labeled at 37 °C in reactions (10 μl) containing 50 mM Tris–HCl, pH 7.6, 10 mM $MgCl_2$, 5 mM dithiotreitol, 0.1 mM spermidine, 10 units T_4 polynucleotide kinase (Fermentas) and 20 μCi [γ^{32}P]ATP (New England Biolabs, 3000 Ci/mmol). Free nucleotides were removed by G25 spin column chromatography.

2.8. Electrophoretic mobility shift assays (EMSA)

Binding reactions (20 μl) contained 20 mM Tris–HCl, pH 7.5, 1 mM dithiotreitol, 1 mM $MgCl_2$, 50 mM KCl, 1 mM EDTA, 12% v/v glycerol, 1 ng 61-bp ^{32}P-heteroduplex, 0.1 μg/ml of a BstEII digest of bacteriophage λ DNA (Promega) as nonspecific competitor and 120 μg yeast protein extract. After incubation for 60 min on ice, reactions were stopped by adding 1 μl of 30% (v/v) glycerol, 0.25% xylene cyanol, 0.25% bromophenolblue and loaded immediately onto a 5% native polyacrylamide gel (acrylamide:bisacrylamide 29:1). Gels were electrophoresed at 10 V/cm in 44.5 mM Tris–borate, pH 7.5, 1 mM EDTA at 4 °C. ^{32}P-labeled complexes were visualized by autoradiography after drying.

2.9. Analysis of Can^r mutation spectra

Individual Can^r colonies from E134 strains transformed with YEp181SPGAL or YEp-AtMSH7/AtMSH2 vectors were replica plated on selective SCDL-agar plates without arginine but containing canavanine. Each colony was then inoculated into 1.5 ml of SCDL liquid media and allowed to grow at 30 °C for 2 days. The cells were harvested by centrifugation, and the resulting cell pellet was resuspended in 50 μl STES buffer (200 mM Tris–HCl, pH 7.6, 500 mM NaCl, 0.1% p/v SDS, 10 mM EDTA) and disrupted with glass beads (Sigma). Afterwards, 20 μl TE (10 mM Tris–HCl, pH 7.6, 1 mM EDTA) and 60 μl phenol:chloroform (1:1) were added. Samples were mixed by brief vortexing and aqueous phases were segregated by 10 min centrifugation (21,000 × *g*). Aqueous phases were transferred to new tubes. Samples were then extracted with an equal volume of chloroform. After extraction, 100% isopropanol was added for DNA precipitation. DNA was pelleted, dissolved in 40 μl water and used as template for PCR amplification of *CAN1* gene. A 1386-bp fragment containing the upstream sequence of *CAN1* was amplified with Up-forward (5′-GTTCTTCAGACTTCTTAACTCCTG-3′) and Up-reverse (5′-CACCAGTAGATGTCTCCATG-3′) primers and a 1438-bp fragment containing the downstream sequence of *CAN1* was amplified with Down-forward (5′-CATATTCTGTCACGCAGTCC-3′) and Down-reverse (5′-CTTATGAGGGTGAGAATGCG-3′) primers. The PCR amplification reaction contained 1 μl genomic DNA, 0.5 μM each gene specific primer, 0.2 mM dNTPs, 0.025 units of GoTaq DNA polymerase (Promega), 4 mU Pfu DNA polymerase (Promega) and 1× GoTaq Reaction Buffer in a final volume of 50 μl. The amplification procedure included an initial denaturation of 7 min at 94 °C followed by a touch-down PCR consisting of 60 s denaturation at 94 °C, 30 s annealing starting at 60 °C, and 135 s extension at 72 °C. The annealing temperature was lowered 2 °C every fifth cycle until it reached 50 °C. After the touch down, the annealing temperature was held at 50 °C for another 30 cycles. The final extension step was at 72 °C for 7 min. Mutation spectra was analyzed by sequencing to determine the inactivating mutation in the *CAN1* gene. Primers used for sequencing were Up-forward, Up-reverse, Down-forward, Down-reverse, Up-OP (5′-GTGCGGCCAATGGTTACATG-3′) and Down-OP (5′-GCTATTGAGAACTCTGGTAC-3′). All DNA sequencing was performed at Macrogen, Korea. Appendix A shows primers used to amplify and sequence the *can1* allele from canavanine-resistant colonies.

3. Results

3.1. Expression constructs

The coding regions of *A. thaliana* MSH7 and MSH2 were cloned in YEp181SPGAL downstream *GAL1* and *GAL10* promoters, respectively (Fig. 1). These constructs were transformed in the MMR-proficient E134 and in the *msh2*Δ derivative of E134 (DAG60) haploid strains. Expression of MMR proteins was then analyzed by SDS-PAGE followed by immunoblotting and detected with purified recombinant anti-AtMSH2 antibodies [23]. As shown in Fig. S1, the recombinant proteins were expressed after 16 h induction with 2% (p/v) galactose at 30 °C. To check if AtMSH2 was properly expressed and stable in yeast cells and since antibodies specific for AtMSH7 are not available, we tested the activity of AtMutSγ by electrophoretic mobility shift experiments.

3.2. Functional analysis of AtMutSγ

We used an electrophoretic mobility shift assay to determine whether MutSγ protein expressed in yeast is functional. As observed in Fig. 2, extracts of MMR proficient (E134) and deficient (DAG60) cells expressing both AtMSH2 and AtMSH7 bind a G-T

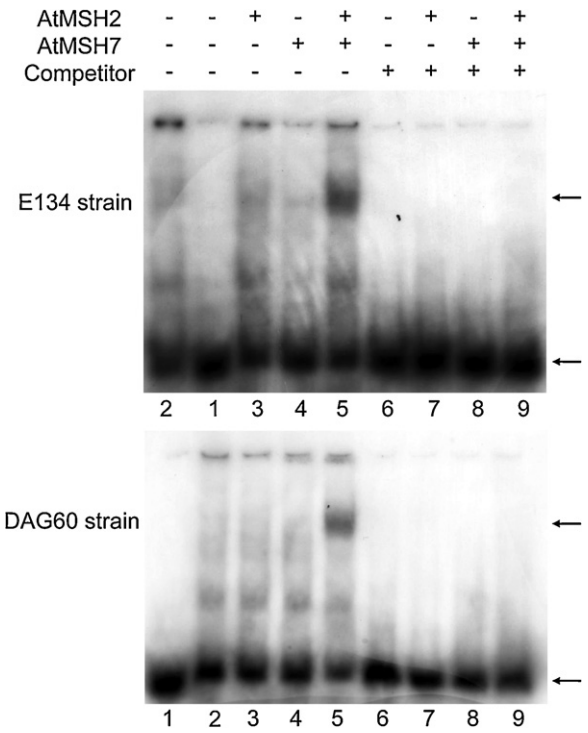

Fig. 2. AtMutSγ binds heteroduplex DNA. Electrophoretic mobility shift analysis of protein–DNA complexes was performed as described under Section 2 with a 61-bp [^{32}P] G-T heteroduplex, BstEII digest of bacteriophage λ DNA as nonspecific competitor and extracts prepared from a MMR proficient (E134, upper panel) or *msh2* mutant (DAG60, lower panel) strains containing control vector (lanes 2 and 6) or expressing individual AtMSH2 (lanes 3 and 7), AtMSH7 (lanes 4 and 8) or co-expressing both subunits (lanes 5 and 9). Protein–DNA complexes were competed out with a 100-fold molar excess of unlabelled oligonucleotide (lanes 6–9). Lane 1: free probe. Specific complexes and free probe are indicated by arrows.

heteroduplex (upper and lower panels, lane 5). Addition of a 100-fold molar excess of unlabelled heteroduplex competitor greatly reduced the specific complex (Fig. 2, upper and lower panels, lane 9). None of the extracts prepared from strains containing control vector or expressing individual AtMSH2 or AtMSH7 displayed detectable oligonucleotide binding (Fig. 2, upper and low panels, lanes 2–4). Thus, the production of supershifted MutSγ–DNA complex is consistent with the formation of a functional AtMutSγ heterodimer in yeast cells.

3.3. Effect of MutSγ on yeast MMR

Three genetic reporter systems were used to study MutSγ function *in vivo*. These previously described genetic markers [15,28] include reversion of the *his7-2* and *lys2::InsE-A14* alleles and forward mutations to *CAN1* (Table 2). The *his7-2* allele contains a single T/A deletion in a stretch of 8 T/As in the *HIS7* gene [15]. Frameshift reversion enables strains to grow on medium lacking

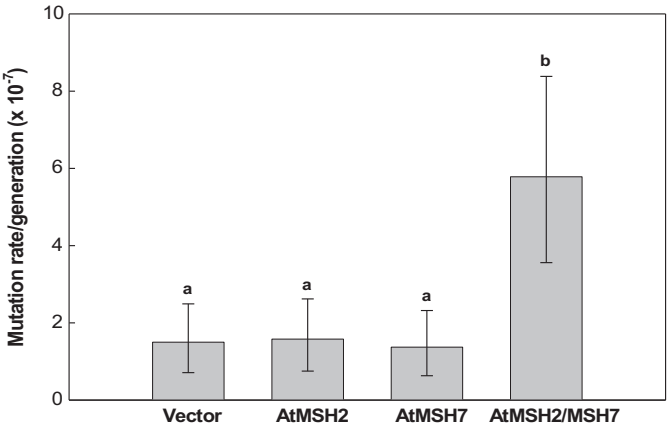

Fig. 3. Effects of AtMSH2 and/or AtMSH7 overexpression on *CAN1* mutation rates. Single transformant colonies of haploid yeast strains E134 containing the empty YEp181SPGAL expression plasmid (vector), YEp181SP-AtMSH2 (AtMSH2), YEp181SP-MSH7 (AtMSH7) and YEp181SPGAL-AtMSH7/AtMSH2 (AtMSH2/MSH7) were grown to saturation in SCDL media, diluted with SCGL and plated after appropriate dilutions onto selective medium lacking arginine but containing canavanine. Data show mean *CAN1* mutation rates values for 5 independent experiments with error bars indicating 95% confidence limits. Different lowercase letters indicate statistical significant differences ($P < 0.05$).

histidine (Table 2). The second assay detects mutations that revert by a single A/T deletion in a mononucleotide run of 14 As in the *LYS2* gene, allowing yeast growth on plates lacking lysine (Table 2). Finally, the *CAN1* forward mutation assay scores a wide variety of base substitutions, frameshifts, and complex mutations (Table 2) that inactivates the arginine permease gene, allowing strains to tolerate media containing canavanine.

Data obtained indicate that AtMSH2 had negligible effects on His$^+$ and Lys$^+$ mutation rates determined by fluctuation analysis (Table 3). Similar results were observed when only AtMSH7 was overexpressed (Table 3). Finally, concomitant overproduction of both AtMSH2 and AtMSH7 subunits yielded rates similar to those observed for the strains overexpressing the individual proteins (Table 3). These data indicate that AtMSH2 and/or AtMSH7 did not affect the reversion rates of *his7-2* and *lys2::InsE-A$_{14}$* alleles when introduced into a MMR proficient yeast strain. Note that the *lys2::InsE-A$_{14}$* mutation system is hypersensitive and detects relatively small mutator effects. We can also infer that AtMSH2 or AtMSH7 in excess do not interfere with yeast MMR system as frameshift mutation rates in the presence of these proteins were unaltered when compared to the control.

We then examined the *CAN1* forward mutation assay. Expression of At*MSH2* or At*MSH7* from *GAL10* or *GAL1* promoters, respectively, resulted in mutation rates indistinguishable from those observed for the vector alone (Fig. 3, 1.58×10^{-7} and 1.37×10^{-7} for At*MSH2* and At*MSH7*, respectively, *vs.* 1.50×10^{-7}). However, MutSγ conferred a 4-fold increase in the mutation rate (Fig. 3, 5.78×10^{-7} *vs.* 1.50×10^{-7}). Although small, this increase was statistically significant as determined by the Mann–Whitney

Table 2
In vivo yeast mutator assays.

Assay	Reporter gene	Region of homonucleotide run	Mutations	Genetic outcome	Phenotypic outcome
Frameshift reversions	*his7-2*	C**AAAAAAA**G G**TTTTTTT**C	(A/T) insertion or (A/T)$_2$ deletion	*HIS7*	His$^+$
	lys2::InsE-A$_{14}$	T**AAAAAAAAAAAAAA**C A**TTTTTTTTTTTTTT**G	(A/T) deletion or (A/T)$_2$ insertion	*LYS2*	Lys$^+$
Forward mutations	*CAN1*	n/a	base substitution, frameshifts, complex mutations	*can1*	Can^r

Can, canavanine; n/a, not-applicable; His$^+$, histidine prototroph; Lys$^+$, lysine prototroph.

Table 3
Effects of AtMSH2 and/or AtMSH7 on mutation rates in homonucleotide runs in MMR proficient strains.

Gene in the YEp181SPGAL vector	His$^+$ reversion rate		Lys$^+$ reversion rate	
	Mutation rate ($\times 10^{-9}$)	CL (95%) [a] ($\times 10^{-9}$)	Mutation rate ($\times 10^{-8}$)	CL (95%) [a] ($\times 10^{-8}$)
None	3.26	1.27–9.94	3.29	0.85–6.79
AtMSH2	3.59	2.12–13.56	4.09	1.16–8.24
AtMSH7	3.03	2.31–12.96	5.71	1.89–10.92
AtMSH2/*AtMSH7*	3.88	0.58–12.97	5.14	1.53–10.17

[a] Confidence limits.

test. For comparison, on average, mutation rate increases of 28- and 13-fold were observed for *msh2* and *msh6* deficient strains compared to MMR proficient strain ([29–32], this work). Thus, overproduction of MutSγ protein only conferred a mild-dominant negative phenotype. Taken together, our results suggest that individual protein subunits do not impair yeast MMR system but overproduction of both AtMSH2 and AtMSH7 form an active MutSγ heterodimer which recognizes a wide variety of DNA lesions scored by canavanine resistance. Such DNA lesion recognition reduces the ability of yeast MutS complexes to interact with DNA substrates. In addition, AtMutSγ seems to be incapable of activating yeast downstream activities and consequently impairs MMR activity.

3.4. Effect of MutSγ on msh2 deficient yeast strains

The roles of AtMSH2 and AtMSH7 in preventing the accumulation of mutations in MMR deficient strains was also examined by the three genetic markers described above (Table 4). These assays demonstrated that the yeast strain containing a deletion in the *MSH2* gene displayed mutation rates 140-, 10,000- and 12-fold higher than wild-type for *HIS7*, *LYS2* and *CAN* markers, respectively (Tables 3 and 4 and Fig. 3). These results are in agreement with previously reported values [16,31,33,34]. This hypermutator phenotype was not affected by the expression of AtMSH2 or AtMSH7 alone or in combination (Table 4). Taken together, our data show that the plasmid overexpressing plant *MSH2* from the *GAL10* promoter does not complement the MMR defect in the *msh2* deletion yeast strain. The MMR deficient mutator phenotype was also unaffected by the expression of AtMSH7 alone or both AtMSH2 and AtMSH7 together.

3.5. Can^r mutation spectrum analysis

The role of AtMutSγ in MMR was initially inferred by determining the mispair recognition of the *in vitro* translated heterodimer using EMSA [5]. However, these studies only analyzed a small number of mutations, limiting the conclusions of these early experiments. To reinvestigate the role of AtMutSγ in MMR, we evaluated the Can^r mutation spectra for E134 strains transformed with the control vector or with the YEp-AtMSH7/AtMSH2 plasmid. Sequence analysis of 21 independent Can^r colonies revealed 25 mutation events in E134 strains containing the control vector (Table 5). We found 15 base-pair substitutions, 7 single base-pair insertions/deletions and 3 complex mutations, which resulted in an occurrence of 0.6 base-pair substitutions, 0.28 single frameshifts and 0.12 complex mutations (Table 5). It should be noted that the Can^r spectra for other wild type strains is quite similar [24,35,36]. These authors observed an occurrence of 0.70, 0.64 and 0.66 of single base substitutions; 0.19, 0.18 and 0.28 of single frameshifts and 0.11, 0.18 and 0.06 of complex mutations.

Sequencing of 21 Can^r isolates from the strain overexpressing AtMutSγ showed 30 mutation events consisting of 26 base-pair substitutions, 3 single base-pair insertions/deletions and 1 complex mutation (Table 5).

From the frequency of each class of mutation and the overall mutation rate of each strain determined by fluctuation analysis, we calculated the Can^r mutation rates for each specific class (Table 5 and Fig. 3). The base substitution rates were 5.03×10^{-7} and 0.90×10^{-7} per generation for the strain transformed with YEp-AtMSH7/AtMSH2 plasmid or containing the control vector, respectively. The rates at which single frameshifts are generated were 0.51×10^{-7} (strain transformed with YEp-AtMSH7/AtMSH2 plasmid) and 0.42×10^{-7} (strain containing the control vector) per cell division while the rates of complex mutations were 0.17×10^{-7} (strain transformed with YEp-AtMSH7/AtMSH2 plasmid) and 0.18×10^{-7} (strain containing the control vector) per generation. These data suggest that AtMutSγ generates a 5-fold increase of single base-pair substitution mutations (Table 5).

We further analyzed the spectrum of base-pair changes and compared the individual base-pair substitution mutations recovered in each strain (Table 5). More transitions and fewer transversions were recovered in E134 strain overexpressing AtMutSγ than in E134 strain containing the control vector. The magnitudes for total transitions were 46% for the strain transformed with YEp-AtMSH7/AtMSH2 plasmid and 33% for the strain containing the control vector, while the magnitudes for total transversions were 54% for the strain transformed with YEp-AtMSH7/AtMSH2 plasmid and 67% for the strain containing the control vector. Data comparison indicates that overexpression of AtMutSγ significantly increased ($P < 0.05$) the relative frequencies of G to A and T to A, C or G substitutions. One hypothesis that explains these results is that AtMutSγ is able to specifically recognize base pair mismatches involved in G:C to A:T and T:A to C:G, G:C or A:T mutations, with subsequent inability of yeast MutS heterodimers to recognize and bind mismatches.

Table 4
Mutation rates of reporter genes under study in *msh2* yeast strains overexpressing *AtMSH2* and/or *AtMSH7*.

Gene in the YEp181SPGAL vector	*his7-2*		*lys2::InsE-A$_{14}$*		*CAN*	
	Mutation rate ($\times 10^{-7}$)	CL (95%) [a] ($\times 10^{-7}$)	Mutation rate ($\times 10^{-4}$)	CL (95%) [a] ($\times 10^{-4}$)	Mutation rate ($\times 10^{-6}$)	CL (95%) [a] ($\times 10^{-6}$)
None	4.62	2.68–6.93	3.40	1.61–5.66	1.81	1.13–2.61
AtMSH2	4.06	2.38–6.04	1.42	0.27–3.16	2.22	1.41–3.16
AtMSH7	3.22	1.80–4.93	1.23	0.19–2.87	2.03	1.22–3.00
AtMSH2/*AtMSH7*	3.43	1.98–5.16	3.04	0.66–6.58	2.25	1.29–3.39

[a] Confidence limits.

Table 5
Spectrum of Can^r mutations.

Strain/plasmid	Type of event	Specific sequence change	Frequency of event		Specific mutation rate ($\times 10^{-7}$)	
E134/vector	Base substitution		0.60 (15/25)		0.90	
		G → A		0.08 (2/25)		0.12
		G → C		0.16 (4/25)		0.24
		G → T		0.08 (2/25)		0.12
		T → A		0 (0/25)		0
		T → C		0 (0/25)		0
		T → G		0.04 (1/25)		0.06
		A → T		0.04 (1/25)		0.06
		A → C		0 (0/25)		0
		A → G		0.04 (1/25)		0.06
		C → A		0.04 (1/25)		0.06
		C → T		0.04 (1/25)		0.06
		C → G		0.08 (2/25)		0.12
	One-base pair frameshift		0.28 (7/25)		0.42	
		C3 → C4		0.04 (1/25)		0.06
		A1 → A0		0.04 (1/25)		0.06
		T6 → T7		0.04 (1/25)		0.06
		T3 → T2		0.04 (1/25)		0.06
		A6 → A5		0.08 (2/25)		0.12
		T3 → T2		0.04 (1/25)		0.06
	Complex		0.12 (3/25)		0.18	
		5-bp duplication		0.04 (1/25)		0.06
		6-bp deletion		0.04 (1/25)		0.06
		38-bp duplication		0.04 (1/25)		0.06
E134/AtMSH2–AtMSH7	Base substitution		0.87 (26/30)		5.03	
		G → A		0.23 (7/30)		1.33
		G → C		0.10 (3/30)		0.58
		G → T		0.03 (1/30)		0.17
		T → A		0.10 (3/30)		0.58
		T → C		0.10 (3/30)		0.58
		T → G		0.13 (4/30)		0.77
		A → T		0.03 (1/30)		0.17
		A → C		0.03 (1/30)		0.17
		A → G		0 (0/30)		0
		C → A		0.07 (2/30)		0.40
		C → T		0.03 (1/30)		0.17
		C → G		0 (0/30)		0
	One-base pair frameshift		0.10 (3/30)		0.51	
		A6 → A5		0.03 (1/30)		0.17
		C1 → C0		0.03 (1/30)		0.17
		A2 → A3		0.03 (1/30)		0.17
	Complex		0.03 (1/30)		0.17	
		7-bp insertion		0.03 (1/30)		0.17

4. Discussion

In the present study, we have used genetic and biochemical approaches to investigate the role of plant MutSγ in mismatch repair. The *A. thaliana* MSH2–MSH7 complex was overexpressed in MMR-proficient and deficient yeast cells. Synthesis of AtMSH2 was revealed by western-blot analysis using anti-AtMSH2 antibodies while expression and proper folding of both AtMSH2 and AtMSH7 was observed by EMSA. We show that AtMutSγ binds DNA containing a G-T mismatch. Extracts of yeast cells overexpressing AtMSH2 or AtMSH7 alone were not able to band-shift the heteroduplex. These data indicate that AtMutSγ protein complex retains mismatch binding activity in yeast cells. Similar G-T heteroduplex binding activity has been reached with AtMSH2 and AtMSH7 proteins, obtained from *in vitro* transcription and translation experiences [5].

Elucidation of the *in vivo* function of AtMutSγ was performed in yeast by using His$^+$ and Lys$^+$ reversion assays and a *CAN1* forward mutation reporter system. When plant AtMSH2 and/or AtMSH7 protein were overexpressed in *msh2* strains the mutator phenotype remained unchanged. These data indicate that AtMSH2 in the presence or absence of its partner AtMSH7 was unable to complement the DNA repair defect of *msh2* cells, probably due to a lack of interaction with heterologous yeast proteins required to complete MMR. Similar to results presented here, Clark et al. [18] reported that human MutSα did not reduce the high reversion rate of the *msh2* mutant strain. In addition, recent research findings in our laboratory determined that expression of AtPMS1 did not affect the mutation rate of a *pms1* deficient strain [37].

On the other hand, we provide evidence that expression of the AtMutSγ protein complex in MMR proficient yeast cells clearly shows a strong preference for mutations scored by the *CAN1* assay but does not change the rates of frameshift reporters. These results agree with observations that indicate a preferential recognition of some base–base mismatches and a weak binding to 1+ T insertion by *in vitro* translated MutSγ protein [5,12]. The increase in the rate of forward mutations at *CAN1* gene reflects a decrease in MMR correction probably due to a reduced binding of yeast MutSα and MutSβ to DNA lesions and the inability of AtMutSγ to interact with yeast downstream proteins. Our results could also suggest a preference of the yeast MMR system for frameshift intermediates over base–base mismatches along with a weak competition of AtMutSγ for the former mutations. In fact, base substitutions were mainly recovered in the wild-type strain, but frameshift mutations predominantly accumulated in the *msh2* strain [29,30,38]. It should be noted that the 4-fold mutator effect of AtMutSγ at the *CAN1* gene is lower than that observed in *msh2* (this work, [29,33]) or *msh6* deficient yeast strains [29,32]. All these findings thus suggest that

expression of AtMutSγ resulted in a partial inactivation of yeast MMR function.

Analysis of Can^r mutation spectra indicated that base pair substitutions are mainly recovered in yeast cells overexpressing AtMutSγ with respect to the control strain. Frequencies of frameshifts and complex mutations are virtually unchanged by the presence of the plant protein. These data confirm the results we obtained with frameshift reporters and indicate that the AtMSH2–AtMSH7 complex functions in the repair of base–base mismatches. The most commonly observed base substitutions were G:C to A:T transitions (23%). Recognized causes for this type of changes are spontaneous deamination of cytosine and 5-methylcytosine, to uracil and thymine, respectively [39]. In plants, 5-methylcytosine residues are found predominantly at symmetric CG and CNG sequences and also at a lower frequency at asymmetric positions such as CNN [40–42]. It is worth mentioning that in plants, cytosine methylation at non-CpG sites occurs much more frequently than in animals [42,43]. G:C to A:T transitions mutations can also be induced by ultraviolet (UV) light at cytosine-containing photoproducts [39,44]. Our results reveal that among the 7 transition mutations observed in strains overexpressing MutSγ, all are in CNN and in dipyrimidine contexts (Appendix A). UV-mutagenesis events also occur at TT sequences, giving a very different mutational pattern. Changes at the 3′ base of a TT site were reported to be predominately T to C transitions and T to A transversions [45]. We also observe a significantly increase of T:A to C:G transitions and T:A to A:T transversions in strains overexpressing AtMutSγ. All T to C mutations were detected at TT sequences and out of de 4 T to A base substitutions 2 were found in TT contexts (Appendix A). Finally, compared to the control, the strain overexpressing MutSγ showed increases in T:A to G:C transversions. This type of base substitution probably reflects mutagenesis caused by endogenous oxidative damage. In fact, deficiency of MutT leads to the enhancement of T:A to G:C transversions more than 1000-fold over the control level in *E. coli* [46]. MutT hydrolyzes 8-oxo-dGTP to 8-oxodGMP and thereby prevents misincorporation of 8-oxo-G opposite A. Interestingly, all land-living plants lack MutT [47].

Collectively, these data suggest that AtMutSγ is able to specifically recognize G/T or A/C mismatches involved in base substitutions of G:C to A:T or T:A to C:G base pairs, T/C or G/A mismatches involved in T:A to G:C transversions and either T/T or A/A mismatches involved in base substitutions of T:A to A:T base pairs. Interestingly, 81% of the base substitutions observed in strains overexpressing AtMutSγ was found next to a T base (either 5′ or 3′) while the control strain did not reflect any preference for DNA sequence contexts.

In conclusion, our work suggests that AtMutSγ could be the protein which recognizes local sequence environments containing T and/or mismatches arisen by deamination of cytosine and 5-methylcytosine and by UV or oxidative mutagenesis. In fact, plants are constantly exposed to DNA damage and thus encode MutSγ as an extra DNA lesion recognition protein to efficiently repair the DNA damage they experience before mutations get fixed to subsequent generations.

Conflict of interest

The authors declare that there are no conflicts of interest.

Acknowledgments

We wish to thank Dmitry Gordenin (National Institute of Environmental Health Sciences, Research Triangle Park, USA) for providing YEp112SPGAL and YEp195SPGAL vectors yeast strains used in recombinant expression experiments and mutation rate determination assays. This work was supported by grants from Agencia Nacional de Promoción Científica y Tecnológica (PICT 0458), Consejo Nacional de Investigaciones Científicas y Técnicas (CONICET; PIP 0018) and Universidad Nacional de Rosario (BIO 221). CPS is a member of the Researcher Career of CONICET.

Appendix A. Supplementary data

Supplementary data associated with this article can be found, in the online version, at http://dx.doi.org/10.1016/j.dnarep.2013.01.002.

References

[1] C.P. Spampinato, R.L. Gomez, C. Galles, L.D. Lario, From bacteria to plants: a compendium of mismatch repair assays, Mutat. Res. Rev. Mutat. Res. 682 (2009) 110–128.
[2] S. Acharya, T. Wilson, S. Gradia, M.F. Kane, S. Guerrette, G.T. Marsischky, R. Kolodner, R. Fishel, hMSH2 forms specific mispair-binding complexes with hMSH3 and hMSH6, Proc. Natl. Acad. Sci. U.S.A. 93 (1996) 13629–13634.
[3] E. Alani, The *Saccharomyces cerevisiae* Msh2 and Msh6 proteins form a complex that specifically binds to duplex oligonucleotides containing mismatched DNA base pairs, Mol. Cell. Biol. 16 (1996) 5604–5615.
[4] J. Genschel, S. Littman, J. Drummond, P. Modrich, Isolation of MutSβ from human cells and comparison of the mismatch repair specificities of MutSβ and MutSα, J. Biol. Chem. 273 (1998) 19895–19901.
[5] K. Culligan, J. Hays, *Arabidopsis* MutS homologs-AtMSH2, AtMSH3, AtMSH6, and a novel AtMSH7-form three distinct protein heterodimers with different specificities for mismatched DNA, Plant Cell 12 (2000) 991–1002.
[6] F. Palombo, I. Iaccarino, E. Nakajima, M. Ikejima, T. Shimada, J. Jiricny, hMutSß, a heterodimer of hMSH2 and hMSH3, binds to insertion/deletion loops in DNA, Curr. Biol. 6 (1996) 1181–1184.
[7] R. Johnson, G. Kovvali, L. Prakash, S. Prakash, Requirement of the yeast MSH3 and MSH6 genes for MSH2-dependent genomic stability, J. Biol. Chem. 271 (1996) 7285–7288.
[8] J.J. Warren, T.J. Pohlhaus, A. Changela, R.R. Iyer, P.L. Modrich, L.S. Beese, Structure of the human MutSα DNA lesion recognition complex, Mol. Cell 26 (2007) 579–592.
[9] G. Obmolova, C. Ban, P. Hsieh, W. Yang, Crystal structures of mismatch repair protein MutS and its complex with a substrate DNA, Nature 407 (2000) 703–710.
[10] M. Lamers, A. Perrakis, J. Enzlin, H. Winterwerp, N. de Wind, T. Sixma, The crystal structure of DNA mismatch repair protein MutS binding to a G-T mismatch, Nature 407 (2000) 712–717.
[11] S.D. Lee, J.A. Surtees, E. Alani, *Saccharomyces cerevisiae* MSH2–MSH3 and MSH2–MSH6 complexes display distinct requirements for DNA binding domain I in mismatch recognition, J. Mol. Biol. 366 (2007) 53–66.
[12] S.-Y. Wu, K. Culligan, M. Lamers, J. Hays, Dissimilar mispair-recognition spectra of *Arabidopsis* DNA-mismatch-repair proteins MSH2*MSH6 (MutSα) and MSH2*MSH7 (MutSγ), Nucleic Acids Res. 31 (2003) 6027–6034.
[13] C. Dong, R. Whitford, P. Langridge, A DNA mismatch repair gene links to the *Ph2* locus in wheat, Genome 45 (2002) 116–124.
[14] A.H. Lloyd, A.S. Milligan, P. Langridge, J.A. Able, *TaMSH7*: a cereal mismatch repair gene that affects fertility in transgenic barley (*Hordeum vulgare* L.), BMC Plant Biol. 7 (2007) 67.
[15] P. Shcherbakova, T. Kunkel, Mutator phenotypes conferred by MLH1 overexpression and by heterozygosity for mlh1 mutations, Mol. Cell. Biol. 19 (1999) 3177–3183.
[16] H.T. Tran, J.D. Keen, M. Kricker, M.A. Resnick, D.A. Gordenin, Hypermutability of homonucleotide runs in mismatch repair and DNA polymerase proofreading yeast mutants, Mol. Cell. Biol. 17 (1997) 2859–2865.
[17] C. Chen, B.J. Merrill, P.J. Lau, C. Holm, R.D. Kolodner, *Saccharomyces cerevisiae* pol30 (proliferating cell nuclear antigen) mutations impair replication fidelity and mismatch repair, Mol. Cell. Biol. 19 (1999) 7801–7815.
[18] A. Clark, M. Cook, H. Tran, D. Gordenin, M. Resnick, T.A. Kunkel, Functional analysis of human MutSα and MutSβ complexes in yeast, Nucleic Acids Res. 27 (1999) 736–742.
[19] F. Sherman, G. Fink, C. Lawrence, Methods in Yeast Genetics, Cold Spring Harbor Laboratory Press, Cold Spring Harbor, NY, 1974.
[20] K. Culligan, J. Hays, DNA mismatch repair in plants. An *Arabidopsis thaliana* gene that predicts a protein belonging to the MSH2 subfamily of eukaryotic MutS homologs, Plant Physiol. 115 (1997) 833–839.
[21] M. Suga, T. Hatakeyama, High-efficiency electroporation by freezing intact yeast cells with addition of calcium, Curr. Genet. 43 (2003) 206–211.
[22] W.N. Burnette, Western blotting: electrophoretic transfer of proteins from sodium dodecyl sulfate-polyacrylamide gels to unmodified nitrocellulose and radiographic detection with antibody and radioiodinated protein A, Anal. Biochem. 112 (1981) 195–203.
[23] R.L. Gomez, C. Galles, C.P. Spampinato, High-level production of MSH2 from *Arabidopsis thaliana*: a DNA mismatch repair system key subunit, Mol. Biotechnol. 47 (2011) 120–129.

[24] G.I. Lang, A.W. Murray, Estimating the per-base-pair mutation rate in the yeast *Saccharomyces cerevisiae*, Genetics 178 (2008) 67–82.
[25] B.M. Hall, C.X. Ma, P. Liang, K.K. Singh, Fluctuation analysis CalculatOR: a web tool for the determination of mutation rate using Luria-Delbruck fluctuation analysis, Bioinformatics 25 (2009) 1564–1565.
[26] P.L. Foster, Methods for determining spontaneous mutation rates, Methods Enzymol. 409 (2006) 195–213.
[27] W.A. Rosche, P.L. Foster, Determining mutation rates in bacterial populations, Methods 20 (2000) 4–17.
[28] K. Drotschmann, A.B. Clark, H.T. Tran, M.A. Resnick, D.A. Gordenin, T.A. Kunkel, Mutator phenotypes of yeast strains heterozygous for mutations in the MSH2 gene, Proc. Natl. Acad. Sci. U.S.A. 96 (1999) 2970–2975.
[29] G. Marsischky, N. Filosi, M. Kane, R. Kolodner, Redundancy of *Saccharomyces cerevisiae* MSH3 and MSH6 in MSH2-dependent mismatch repair, Genes Dev. 10 (1996) 407–410.
[30] D. Tishkoff, N. Filosi, G. Gaida, R. Kolodner, A novel mutation avoidance mechanism dependent on *S. cerevisiae* RAD27 is distinct from DNA mismatch repair, Cell 88 (1997) 253–263.
[31] K. Drotschmann, W. Yang, T.A. Kunkel, Evidence for sequential action of two ATPase active sites in yeast Msh2–Msh6, DNA Repair 1 (2002) 743–753.
[32] J.M. Harrington, R.D. Kolodner, *Saccharomyces cerevisiae* Msh2–Msh3 acts in repair of base–base mispairs, Mol. Cell. Biol. 27 (2007) 6546–6554.
[33] D.X. Tishkoff, N. Filosi, G.M. Gaida, R.D. Kolodner, A novel mutation avoidance mechanism dependent on *S. cerevisiae* RAD27 is distinct from DNA mismatch repair, Cell 88 (1997) 253–263.
[34] P. Shcherbakova, M. Hall, M. Lewis, S. Bennett, K. Martin, P. Bushel, C. Afshari, T. Kunkel, Inactivation of DNA mismatch repair by increased expression of yeast MLH1, Mol. Cell. Biol. 3 (2001) 940–951.
[35] M.-E. Huang, A.-G. Riot, A. Nicolas, R.D. Kolodner, A genomewide screen in *Saccharomyces cerevisiae* for genes that suppress the accumulation of mutations, Proc. Natl. Acad. Sci. U.S.A. 100 (2003) 11529–11534.
[36] M.-E. Huang, A.-G. Rio, M.-D. Galibert, F. Galibert, Pol32, a subunit of *Saccharomyces cerevisiae* DNA polymerase δ, suppresses genomic deletions and is involved in the mutagenic bypass pathway, Genetics 160 (2002) 1409–1422.
[37] C. Galles, C. Spampinato, Yeast mutator phenotype enforced by Arabidopsis PMS1 expression, Mol. Biol. Rep. (2012), http://dx.doi.org/10.1007/s11033-11012-12269-11035.
[38] M. Huang, A. Rio, M. Galibert, F. Galibert, Pol32, a subunit of *Saccharomyces cerevisiae* DNA polymerase delta, suppresses genomic deletions and is involved in the mutagenic bypass pathway, Genetics 160 (2002) 1409–1422.
[39] S. Ossowski, K. Schneeberger, J.I. Lucas-Lledó, N. Warthmann, R.M. Clark, R.G. Shaw, D. Weigel, M. Lynch, The rate and molecular spectrum of spontaneous mutations in *Arabidopsis thaliana*, Science 327 (2010) 92–94.
[40] Y. Gruenbaum, R. Naveh-Many, H. Cedar, A. Razin, Sequence specificity of methylation in higher plant DNA, Nature 292 (1981) 860–862.
[41] P. Meyer, I. Niedenhof, M.T. Lohuis, Evidence for cytosine methylation of non-symmetrical sequences in transgenic *Petunia hybrida*, EMBO J. 13 (1994) 2084–2088.
[42] B.F. Vanyushin, DNA methylation in plants, Curr. Top. Microbiol. Immunol. 301 (2006) 67–122.
[43] R.A. Martienssen, V. Colot, DNA methylation and epigenetic inheritance in plants and filamentous fungi, Science 293 (2001) 1070–1074.
[44] E.C. Friedberg, G.C. Walker, W. Siede, R.D. Wood, R.A. Schultz, T. Ellenberge, DNA Repair and Mutagenesis, American Society for Microbiology Press, Washington, DC, 2006.
[45] W.B. Mak, D. Fix, DNA sequence context affects UV-induced mutagenesis in *Escherichia coli*, Mutat. Res. 638 (2008) 154–161.
[46] M. Sekiguchi, MutT-related error avoidance mechanism for DNA synthesis, Genes Cells 1 (1996) 139–145.
[47] K. Jansson, A. Blomberg, P. Sunnerhagen, M. Alm Rosenblad, Evolutionary loss of 8-oxo-G repair components among eukaryotes, Genome Integr. 1 (2010) 12.